Griffis, N.P., et al., 2019, Coupled stratigraphic and U-Pb zircon age constraints on the late Paleozoic icehouse-to-greenhouse turnover in south-central Gondwana: Geology, v. 47, https://doi.org/10.1130/G46740.1

Appendix

Existing U-Pb Geochronologic Framework for Paraná and Karoo basins

Numerous recent studies have placed age control on the ice-proximal deposits of the late Paleozoic successions in the Paraná and Karoo basins by means of radioisotopic analyses (Bangert et al., 1999; Guerra-Sommer et al., 2008a, 2008b, 2008c; Stollhofen et al., 2008; Mori et al., 2012; Cagliari et al., 2014; McKay et al., 2015; Cagliari et al., 2016). Recent high-resolution U-Pb zircon chemical abrasion thermal ionizing mass spectrometry (CA-TIMS) of tonsteins, weathered volcanic ash found in coal, refines the previous stratigraphy of the southern Paraná Basin and highlights the impact of Pb-loss and complex age inventories on assigning U-Pb ages (Griffis et al., 2018). Here we review the established stratigraphy and the associated published radioisotope age constraints for the Paraná and Karoo basins.

Paraná Basin

A wealth of multi-crystal batch and single crystal zircon ages have been produced for the Rio Bonito Fm. volcaniclastic deposits over the last two decades (*summarized in* Griffis et al., 2018). Recent high-resolution U-Pb zircon CA-TIMS analysis of tonsteins in Rio Grande do Sul State (S Brazil), which overlie the glacial deposits of the Itararé Gp. indicate termination of glaciation in the southern Paraná Basin prior to and proximal to the Carboniferous-Permian boundary (Table 1A; Griffis et al., 2018; CT1 - 298.23 ±0.31 Ma). Additional ashes in the Candiota region (CT3 - 297.58 +0.68/-1.4 Ma and HNC - 297.77 +0.35/-0.59 Ma) and from an isolated outcrop 140 km to the north of the Candiota region (QUT - 296.97 +0.45/-0.72 Ma) further argue for a Carboniferous age for terminal deglaciation in the southern Paraná Basin (Fig. 1; Griffis et al., 2018). Reanalysis of the

Faxinal coal tonstein, which had previously been suggested to be coeval with the Candiota deposits, yields a U-Pb zircon CA-TIMS age at least 10 Ma younger (FAX - 285.42 +1.2/-2.1 Ma; Griffis et al., 2018). An existing SIMS U-Pb age for the Recreio Mine tonstein, which is located in the upper Rio Bonito Fm., also indicates a younger age (291 ±1.3 Ma) than the Candiota coals (Simas et al., 2012). This study reanalyzes the Recreio Mine tonstein by CA-TIMS.

Karoo Basin

Late Paleozoic deglaciation sequences, defined as clast-rich diamictite, overlain by clast-poor sandstones or mudstones, were described by Visser (1997) and have been correlated across the Karoo and Kalahari basins (Visser, 1997; Stollhofen et al., 2008). Several U-Pb zircon studies of the late Paleozoic deglaciation sequences of the Karoo and Kalahari basins of South Africa and Namibia, respectively, have been conducted over the last two decades (Bangert et al., 1999; Stollhofen et al., 2008; McKay et al., 2015). All of the U-Pb ages presented in these aforementioned studies were measured using secondary ion mass spectrometry (SIMS). U-Pb ages for deglaciation sequence II (DS II) range from 302 ±3.0 to 299.2 ±3.2 Ma in the Kalahari Basin (Bangert et al., 1999). An age of 297 ±1.8 Ma is reported for DS III in the Karoo Basin, South Africa (Bangert et al., 1999). U-Pb zircon ages for the terminal deglaciation in the Karoo Basin come from the basal Ecca Gp. (Prince Albert Fm.) and range from 289.6 ±3.8 Ma to 288.5 ±1.6 Ma (Bangert et al., 1999; Stollhofen et al., 2008). In Namibia, U-Pb zircon ages for the basal Ecca Gp. are reported as 290.9 ±1.7 Ma (Stollhofen et al., 2008). All U-Pb SIMS ages reported from the Karoo and Kalahari basins reveal significant age dispersion indicating that the U-Pb zircon framework for the late Paleozoic successions across these regions may be affected by Pb-

47 loss, multiple episodes of zircon growth or are the result of cryptic older cores (summarized
48 in Griffis et al., 2018).
49
50 **New U-Pb Zircon Geochronology**
51 We report new high-resolution U-Pb zircon CA-TIMS ages for newly discovered as well
52 as previously dated volcaniclastic deposits in the Paraná and Karoo basins (Table A1 and
53 Table A2). Here we present the individual single zircon crystal U-Pb CA-TIMS analytical
54 results, the interpreted depositional ages, concordia plots, and rank order plots for all
55 samples (Table A1, Table A2; Fig., A1, Fig. A2). The age inventory for all samples is
56 complex which we attribute to the presence of xenocrystic zircons, the inclusion of relict
57 inherited core material in individual zircon crystals, and/or suspected Pb-loss (Fig. A1 and
58 A2). In order to curtail *suspected* Pb-loss, multiple chemical treatments, which include an
59 8-hour and 12-hour chemical abrasion, were employed with varying degrees of success (cf.
60 KKDDt and ANT1). The extraction of eruption/depositional ages of such suites is not
61 straight forward, therefore we report three different approaches for the age interpretation
62 that include (1) the weighted mean of the youngest coherent group of grains, (2) the
63 youngest zircon algorithm (Isoplot 3.1; *see* Griffis et al., 2018), and (3) a Bayesian model
64 age calculated using a triangular prior (Keller et al., 2018). The youngest zircon algorithm
65 and the Bayesian model ages are favored where the age dispersion towards the younger
66 end member cannot be interpreted as Pb-loss (Table A1; *see* Griffis et al., 2018; Keller et
67 al., 2018). Although these two approaches typically result in slightly elevated uncertainty,
68 they arguably provide a more geologically realistic interpretation of the depositional age,
69 in contrast to the more precise weighted mean age (*see* Griffis et al., 2018; Keller et al.,

2018). Importantly, for coherent suites of zircon ages within one sample, all three ages overlap within uncertainty at the 2σ-level.

Paraná Basin

Anitápolis Poço (Lat. 27° 50.359'S; Long. 49° 14.217'W)

The Anitápolis Poço Ash (ANT1) was obtained from core 7RL-04-SC-02, which was drilled near the town of Anitápolis, Santa Catarina State (SE Paraná Basin). The ash was sampled from the Triunfo Mbr. of the Rio Bonito Fm. and is located 67 m above the glaciogenic deposits of the Itararé Gp. A total of 30 single crystal zircon ages were analyzed for the ANT1 sample. The initial batch of 23 single crystal zircons was analyzed following an 8-hr chemical abrasion at 220°C. One sample was discordant and rejected. An additional six zircons produced Ordovician and Cambrian ages. The remaining zircons yielded ages ranging from the late Carboniferous though early Permian (Fig. A2). An additional seven zircons were measured following a 12-hour chemical abrasion at 220°C. One zircon grain reproduced the earliest Permian age. We calculate youngest zircon ages of 296.5 +2/-1.8 Ma (ET535 Spike) and 296.13 +1.5/-2 Ma (BGC 535 Spike) using the youngest zircon algorithm in Isoplot 3.1. The youngest three grains analyzed from this sample have relatively large individual uncertainties which may mask Pb-loss. A weighted mean age of 298.72 ±0.68 Ma (MSWD = 1.3; BGC 535 Spike) is calculated from the youngest coherent subset that rejects the three youngest grains with large individual uncertainties on the basis of masking suspected Pb-loss. To avoid the possibility of rejecting grains on the basis of *suspected* Pb-loss we elected to report a Bayesian model age of 297.4 +1.13/-1.19 Ma that incorporated all Carboniferous-Permian age grains (Table A1; *see* Keller et al., 2018). This

age overlaps within uncertainty of the weighted mean and the youngest zircon age. Furthermore, this Bayesian model age is consistent with other ages from similar stratigraphic positioning in the southern Paraná Basin.

Alfredo Wagner Ash (Lat. 27° 43.974'S Long. 49° 22.199'W)

The Alfredo Wagner ash (AWT) was sampled from a thin white layer (~2 cm) that occurs between two sandstone beds, along a roadside outcrop outside the town of Alfredo Wagner, Santa Catarina State (SE Brazil). Seven zircons were analyzed following an 8-hour abrasion at 220°C. Five zircons produce ages ranging from Paleoproterozoic through Cambrian. Two zircons reproduce early Permian ages (Fig. A2). We calculate an age of 294.77 +0.72/-0.67 Ma using the youngest zircon algorithm. In addition, we report a Bayesian model age of 294.82 +0.59/-0.83 Ma, consistent with the latter age, which we interpret as the age of this deposit (Table A1). Due to the limited number of analysis from this sample as a result of limited sample material, this age should be used cautiously as younger grains may exist but may not be represented in the analyzed zircons.

Recreio Mine Tonstein (Lat. 30° 6.503'S long. 51° 56.283'W)

The Recreio Mine tonstein (RMT) was sampled from a thin (~2 cm) white volcanic layer identified in the S1 coal seam within the Rio Bonito Fm. of the Recreio Mine, which is located outside the town of Leão-Butiá, Rio Grande do Sul State. We sampled from the same layer as Simas et al., (2012). A total of fourteen zircons from the Recreio Mine were analyzed. Eight zircon grains were subject to an 8-hour chemical abrasion at 220°C; one zircon produced a slightly younger age of 288 Ma compared to the other zircons of the group that produced ages of 290 to 291 Ma. An additional six zircons were subjected to a

longer 12-hour chemical abrasion at 220°C, after which one grain was discordant, another produced a spurious 302 Ma age, and the remaining four grains cluster around 291 Ma (Fig. A2). A weighted mean of the four youngest zircons following the 12-hour abrasion produce an age of 291.03 ±0.26 Ma (MSWD = 0.19). In addition, we report a Bayesian model age of 290.36 +0.4/-0.32 Ma which we interpret as the age of this deposit (Table A1).

Karoo Basin

Klaarstroom (Lat. 33° 8.701'S Long. 22° 32.796'E)

The Klaarstroom ash (KKDDt) was collected outside of the town of Klaarstroom, western Cape Province of the Republic of South Africa. KKDDt was sampled from the same pebbly mudstone outcrop where samples for published SIMS-based U-Pb ages were obtained (Fig. 1; Bangert et al., 1999). This interval corresponds to DS III (Bangert et al., 1999; Stollhofen et al., 2008). A total of twenty zircons were analyzed. Twelve zircons were subjected to an 8-hour chemical abrasion at 220°C and exhibit minor age dispersion, possibly a result of Pb-loss. In order to minimize suspected Pb-loss, a more aggressive 12-hour chemical abrasion at 220°C was employed on eight additional zircons which display less age dispersion (Fig A2). One zircon was discordant and rejected from the analysis. The weighted mean of the youngest four zircons from the 12-hour abraded crystals produced an age of 296.30 ± 0.49 Ma (MSWD = 1.8). An age of 295.97 + 0.36/-0.66 Ma is calculated using the youngest zircon algorithm. The weighted mean age and the youngest zircon age overlap within uncertainty of our Bayesian model age of 296.41 +0.27/-0.35 Ma which we interpret as the age of this deposit (Table A1).

Laingsburg

DPAL2 (Lat. 33° 16.855'S Long. 20° 55.005'E)

The DPAL 2 ash was collected from roadside outcrop outside the town of Laingsburg, in the western Cape Province of South Africa. DPAL2 was sampled in a tightly folded mudstone outcrop of the Ecca Gp. (Prince Albert Fm.) above the glacial sequences of the Dwyka Gp. (DS IV). The DPAL2 ash was sampled from the same outcrop where published SIMS-based U-Pb ages were obtained (Bangert et al., 1999). A total of twelve zircons were analyzed following a 12-hour chemical abrasion at 220°C all of which are analytically concordant. Seven grains reproduce at ~284 Ma, two reproduce at ~283 and three additional grains reproduce at ~282 Ma (Fig. A2). One grain reproduced well outside the uncertainty of all other grains at 274 Ma and is interpreted as Pb-loss. The three youngest grains produce a weighted mean age of 282.15 ±0.25 Ma (MSWD = 1.06). Since Pb loss is present we cannot rule out the possibility of Pb-loss affecting this age. An age of 281.9 +0.34/-0.59 Ma is calculated using the youngest zircon algorithm. The weighted mean age and the youngest zircon age overlap within uncertainty of our Bayesian model age of 282.17 +0.32/-0.44 Ma and is interpreted as the age of this deposit (Table A1).

KDPA63 (Lat. 33° 14.397'S Long. 20° 51.985'E)

The KDPA63 ash was sampled outside the town of Laingsburg, in a mudstone facies, 63 meters above the contact of the glacial deposits of the Dwyka Gp. and mudstones of the Ecca Gp. (Prince Albert Fm.). The contact with the Dwyka Gp. at this section is conformable. A total of seven zircons were measured following a 12-hour chemical abrasion. The pattern of age dispersion for this sample is similar to DPAL2, with single

crystal U-Pb ages ranging from ~284 to ~280 Ma (Fig A2). A weighted mean age of 281.38 ±0.44 Ma (MSWD = 0.95) is calculated from the two youngest zircons. An age of 280.81 +0.74/-1.3 Ma is calculated using the youngest zircon algorithm. The latter age overlaps within uncertainty with that of the Bayesian model age of 281.15 +0.72/-1.12 Ma, which is interpreted as the age of this deposit (Table A1).

Analytical procedures

Zircons were separated from volcaniclastic material using standard mineral separation techniques, including sieves, magnetic and density separation. Euhedral, clear grains were picked and screened for core using transmitted and polarized light. Crystals with optically recognizable cores were discarded, though older cryptic cores often escape detection in a petrographic microscope, and as a result may contribute to the age dispersion observed in samples analyzed in this study. All zircons were pretreated using thermal annealing at 900°C for 48 hrs, followed by chemical abrasion (Mattinson, 2005) with concentrated HF in pressurized dissolution capsules at 220°C for 8 to 12 hrs. Prior to dissolution the crystals were cleaned in ultrasonically agitated aqua regia followed by multiple steps of rinsing in clean HNO_3. Zircon crystals were then spiked with either the EarthTime 535 (ET 535) or Berkeley Geochronology Center (BGC 535) ^{205}Pb-^{233}U-^{235}U tracer solution and dissolved by vapor transfer in HF using miniature PTFE capsules at 220°C for 6 days (Table A2). Isotope ratios were determined on a Micromass Sector 54 mass spectrometer using a Daly-type ion counter positioned behind a WARP filter. Pb (as Pb^{+}) and U (as UO^{2+}) were run sequentially on the same filament. The accuracy of the BGC 535 mixed tracer was tested repeatedly against solutions derived from certified standards of isotopically pure ^{206}Pb and natural U (NIST SRM-991 and CRM-145, respectively), as well as age solutions

distributed by the EarthTime initiative (agreement was found to be <0.1%, additional details regarding tracer calibration are in Griffis et al., 2018; Irmis et al., 2011; Mundil et al., 2004; Black et al., 2004). Repeat measurements of the total procedural blank averaged 0.82 ± 0.36 pg Pb (U blanks were indistinguishable from zero), with $^{206}Pb/^{204}Pb$ = 18.40 ± 0.46, $^{207}Pb/^{204}Pb$ = 15.64 ± 0.25, $^{208}Pb/^{204}Pb$ = 38.04 ± 0.75 (all 2σ of population), and a $^{206}Pb/^{204}Pb$-$^{207}Pb/^{204}$ Pb correlation of +0.47 (ratios and uncertainties were propagated into the age and age-error calculations). Deficient radiogenic ^{206}Pb in zircon due to initial deficit of ^{230}Th is accounted for by assuming a partition coefficient ratio DTh/DU of 0.2 (as applied in Wotzlaw et al., 2014). Mass fractionation of U during analysis was controlled by the U double spike, whereas Pb mass fractionation was corrected by 0.15 ± 0.6 %/AMU (based on multiple analyses of NBS 981).

References

Bangert, B., Stollhofen, H., Lorenz, V., and Armstrong, R., 1999, The geochronology and significance of ash-fall tuffs in the glaciogenic Carboniferous-Permian Dwyka Group of Namibia and South Africa: Journal of African Earth Sciences, v. 29, no. 1, p. 33-49.

Black, L.P., Kamo, S.L., Allen, C.M., Davis, D.W., Aleinikoff, J.N., Valley, J.W., Mundil, R., Campbell, I.H., Korsch, R.J., Williams, I.S., and Foudoulis, C., 2004, Improved 206Pb/238U microprobe geochronology by the monitoring of a trace-element-related matrix effect; SHRIMP, ID-TIMS, ELA-ICP-MS and oxygen isotope documentation for a series of zircon standards: Chemical Geology, v. 205, p. 115-140

Cagliari, J., Lavina, E. L. C., Philipp, R. P., Tognoli, F. M. W., Basei, M. A. S., and Faccini, U. F., 2014, New Sakmarian ages for the Rio Bonito formation (Parana Basin, southern Brazil) based on LA-ICP-MS U-Pb radiometric dating of zircons crystals: Journal of South American Earth Sciences, v. 56, p. 265-277.

Cagliari, J., Philipp, R. P., Buso, V. V., Netto, R. G., Hillebrand, P. K., da Cunha Lopes, R., Basei, M. A. S., and Faccini, U. F., 2016, Age constraints of the glaciation in the Paraná Basin: evidence from new U–Pb dates: Journal of the Geological Society, p. jgs2015-2161.

Griffis, N.P., Mundil, R., Montanez, I.P., Isbell, J., Fedorchuk, N., Vesely, F.F., Iannuzzi, R. and Yin, Q.Z., 2018, A new stratigraphic framework built on U-Pb single zircon TIMS ages with implications for the timing of the penultimate icehouse (Paraná Basin, Brazil): Geological Society of America, Bulletin, v. 130 no. 5/6, p. 848-858.

Guerra-Sommer, M., Cazzulo-Klepzig, M., Santos, J. O. S., Hartmann, L. A., Ketzer, J. M., and Formoso, M. L. L., 2008a, Radiometric age determination of tonsteins and stratigraphic constraints for the Lower Permian coal succession in southern Parana Basin, Brazil: International Journal of Coal Geology, v. 74, no. 1, p. 13-27. doi:10.1016/j.coal.2007.09.005.

Guerra-Sommer, M., Cazzulo-Klepzig, M., Menegat, R., Laquintinie Formoso, M. L., Stipp Basei, M. A., Barboza, E. G., and Simas, M. W., 2008b, Geochronological data from the Faxinal coal succession, southern Parana Basin, Brazil: A preliminary approach combining radiometric U-Pb dating and palynostratigraphy: Journal of South American Earth Sciences, v. 25, no. 2, p. 246-256. doi:10.1016/j.jsames.2007.06.007.

Guerra-Sommer, M., Cazzulo-Klepzig, M., Laquintinie Formoso, M. L., Menegat, R., and Mendonca Fo, J. G., 2008c, U-Pb dating of tonstein layers from a coal succession of the southern Parana Basin (Brazil): A new geochronological approach: Gondwana Research, v. 14, no. 3, p. 474-482. doi:10.1016/j.gr.2008.03.003.

Irmis, R.B., Mundil, R., Martz, J.W., and Parker, W.G., 2011, High-resolution U–Pb ages from the Upper Triassic Chinle Formation (New Mexico, USA) support a diachronous rise of dinosaurs: Earth and Planetary Science Letters, v. 309, p. 258-267.

Jaffey, A.H., Flynn, K.F., Glendenin, L.E., Bentley, W.C. and Essling, A.M. , 1971. Precision measurements of half-lives and specific activities of ^{235}U and ^{238}U. Physical Reviews, C4, p, 1889-1906.

Keller, C.B., Schoene, B., Samperton, K., 2018, A stochastic sampling approach to zircon eruption age interpretation: Geochemical Perspectives Letters v. 8, p. 31-35.

Mattinson, J.M., 2005, Zircon U-Pb chemical abrasion ("CA-TIMS") method: Combined annealing and multi-step partial dissolution analysis for improved precision and accuracy of zircon ages: Chemical Geology, v. 220, p. 47-66.

McKay, M. P., Weislogel, A. L., Fildani, A., Brunt, R. L., Hodgson, D. M., and Flint, S. S., 2015, U-PB zircon tuff geochronology from the Karoo Basin, South Africa: implications of zircon recycling on stratigraphic age controls: International Geology Review, v. 57, no. 4, p. 393-410. doi:10.1080/00206814.2015.1008592.

Mori, A. L. O., de Souza, P. A., Marques, J. C., and Lopes, R. d. C., 2012, A new U-Pb zircon age dating and palynological data from a Lower Permian section of the southernmost Parana Basin, Brazil: Biochronostratigraphical and geochronological implications for Gondwanan correlations: Gondwana Research, v. 21, no. 2-3, p. 654-669.

Mundil, R., Ludwig, K.R., Metcalfe, I., and Renne, P.R., 2004, Age and timing of the Permian mass extinctions: U/Pb dating of closed-system zircons: Science, v. 305, p. 1760-1763.

Simas, M. W., Guerra-Sommer, M., Cazzulo-Klepzig, M., Menegat, R., Schneider Santos, J. O., Fonseca Ferreira, J. A., and Degani-Schmidt, I., 2012, Geochronological correlation of the main coal interval in Brazilian Lower Permian: Radiometric dating of tonstein and calibration of biostratigraphic framework: Journal of South American Earth Sciences, v. 39, p. 1-15. doi:10.1016/j.jsames.2012.06.001.

Stollhofen, H., Werner, M., Stanistreet, I. G., and Armstrong, R. A., 2008, Single-zircon U-Pb dating of Carboniferous-Permian tuffs, Namibia, and the intercontinental deglaciation cycle framework, *in* Fielding, C. R., Frank, T. D., and Isbell, J. L., eds., Resolving the Late Paleozoic Ice Age in Time and Space, Volume 441, p. 83-96.

Visser, J. N. J., 1997, Deglaciation sequences in the Permo-Carboniferous Karoo and Kalahari basins of southern Africa: A tool in the analysis of cyclic glaciomarine basin fills: Sedimentology, v. 44, no. 3, p. 507-521.

Wotzlaw, J.-F., Hüsing, S.K., Hilgen, F.J., and Schaltegger, U., 2014, High-precision zircon U–Pb geochronology of astronomically dated volcanic ash beds from the Mediterranean Miocene: Earth and Planetary Science Letters, v. 407, p. 19-34.

Figure Captions

Figure A1. Concordia diagrams for all volcaniclastic samples presented in this study. Error ellipses are 2-sigma.

Figure A2. U-Pb single crystal zircon CA-TIMS ages for the Paraná and Karoo basins. A. U-Pb ages for S Paraná Basin from Griffis et al. (2018). B. New U-Pb zircon CA-TIMS ages for the S, SE Paraná and Karoo basins. Red bars are single zircon crystal U-Pb ages. All ages presented in this study are calculated using a Bayesian Statistical approach (Keller et al., 2018). Superscript numbers are sample locations and relate to numbers in map in Fig. 1. C.

Table A1. Paraná and Karoo basin LPIA U-Pb Zircon CA-TIMS Age Control

Sample Name	Weighted Mean (Ma)	MSWD*	Youngest Zircon (Ma)	Bayesian Age (Ma)
Griffis et al., 2018				
CT1	**298.23 ±0.31**	0.4	–	–
CT3	298.64 ±0.17	1	**297.58 +0.68/-1.4**	–
HNC	298.03 ±0.25	0.3	**297.77 +0.35/-0.59**	–
QUT	298.10 ±0.28	1.5	**296.97 +0.45/-0.72**	–
FAX	285.52 ±0.30	1.2	**285.42 +1.2/-2.1**	–
Present Study				
KKDDt	296.30 ±0.49	1.8	295.97 +0.36/-0.66	**296.41 +0.27/-0.35**
DPAL2	282.15 ±0.25	1.06	281.9 +0.34/ -0.59	**282.17 +0.32/-0.44**
KDPA63	281.38 ±0.44	0.95	280.81 +0.74/ -1.3	**281.15 +0.72/-1.12**
RMT1	291.03 ±0.26	0.19	–	**290.36 +0.4/-0.32**
ANT1	298.72 ±0.68	1.3	296.5 +2/ -1.8	**297.4 +1.13/-1.19**
AWT	–	–	294.79 +0.72/-0.67	**294.82 +0.59/-0.83**

*MSWD - mean square weighted deviates.
Reported age uncertanties are 2-sigma.
Bold values are recommended ages (See data supplement for details).
See data supplement for sample locations.

Table A2 **Isotopic ratios** **Isotopic Age**

Sample	CA	Pbc (pg)$_a$	Th/U $_b$	$^{206}Pb/^{204}Pb$ $_c$	$^{207}Pb/^{235}U$ $_d$	2σ % err	$^{206}Pb/^{238}U$ $_{d,f}$	2σ % err	Corr. coef.	$^{207}Pb/^{206}Pb$ $_{d,f}$	2σ % err	$^{206}Pb/^{238}U$ $_{e,f}$	abs (±2σ)
Karoo Basin													
KKDDt													
z121	12	1.6	0.54	433	0.3391	1.26	0.047240	0.16	0.47	0.05208	1.20	297.55	0.46
z129	12	1.3	0.57	1886	0.3402	0.39	0.047152	0.11	0.53	0.05235	0.34	297.01	0.33
z127	12	1.2	0.52	836	0.3378	0.76	0.047126	0.16	0.50	0.05201	0.70	296.85	0.47
z125	12	1.2	0.51	1121	0.3394	0.57	0.047110	0.21	0.50	0.05227	0.50	296.75	0.60
z126	12	1.7	0.60	947	0.3381	0.69	0.047076	0.16	0.47	0.05211	0.63	296.54	0.47
z128	12	1.0	0.49	1977	0.3378	0.39	0.047005	0.11	0.52	0.05214	0.34	296.11	0.33
z131	12	1.3	0.48	2126	0.3397	0.52	0.046993	0.22	0.56	0.05246	0.44	296.03	0.65
z132	12	1.0	0.65	3193	0.3195	0.39	0.044240	0.24	0.71	0.05240	0.28	279.06	0.66
*z1	8	1.7	0.52	769	0.3500	2.09	0.048071	0.56	0.45	0.05280	1.90	302.67	1.71
*z3	8	1.8	0.52	1025	0.3439	0.61	0.047563	0.24	0.49	0.05244	0.53	299.54	0.71
*z2	8	2.4	0.58	242	0.3407	2.39	0.047254	0.24	0.50	0.05229	2.27	297.64	0.72
*z12	8	0.8	0.52	781	0.3393	0.81	0.047150	0.18	0.41	0.05219	0.75	297.00	0.52
*z10	8	1.0	0.55	1573	0.3399	0.43	0.047114	0.11	0.44	0.05232	0.40	296.78	0.34
*z8	8	1.3	0.62	1761	0.3376	0.36	0.047086	0.11	0.44	0.05200	0.33	296.61	0.33
*z11	8	3.0	0.59	458	0.3401	1.11	0.047084	0.20	0.38	0.05239	1.05	296.60	0.60
*z6	8	0.8	0.56	3219	0.3394	0.26	0.047083	0.16	0.69	0.05228	0.19	296.59	0.47
*z7	8	2.8	0.56	701	0.3394	0.72	0.047041	0.16	0.38	0.05232	0.68	296.33	0.47
*z5	8	1.4	0.56	2061	0.3385	0.37	0.046937	0.14	0.52	0.05230	0.32	295.69	0.43
*z4	8	1.2	0.59	1201	0.3380	0.50	0.046895	0.27	0.60	0.05227	0.40	295.43	0.79
*z9	8	1.2	0.50	2425	0.3378	0.34	0.046774	0.14	0.49	0.05238	0.29	294.68	0.40
DPAL2													
z12	12	1.6	0.50	1183	0.3235	0.84	0.045085	0.35	0.46	0.05206	0.74	284.27	0.98
z8	12	1.0	0.56	745	0.3234	0.76	0.045078	0.13	0.41	0.05206	0.71	284.23	0.35
z4	12	1.0	0.48	1313	0.3239	0.56	0.045061	0.18	0.47	0.05215	0.50	284.13	0.49
z6	12	2.1	0.48	667	0.3219	1.12	0.045060	0.18	0.59	0.05184	1.02	284.12	0.50
z5	12	1.4	0.48	1168	0.3227	0.72	0.045029	0.23	0.52	0.05200	0.63	283.93	0.64
z3	12	1.1	0.48	1116	0.3231	0.56	0.045021	0.13	0.51	0.05208	0.50	283.88	0.35
z7	12	0.8	0.54	946	0.3221	0.64	0.045005	0.17	0.48	0.05193	0.58	283.78	0.48
z1	12	0.9	0.49	1343	0.3221	0.48	0.044881	0.13	0.52	0.05208	0.43	283.02	0.35
z9	12	1.1	0.64	885	0.3210	0.65	0.044766	0.13	0.48	0.05202	0.60	282.31	0.36
z11	12	2.8	0.52	489	0.3196	1.31	0.044736	0.19	0.45	0.05184	1.23	282.12	0.51
z2	12	2.2	0.46	360	0.3206	1.49	0.044695	0.18	0.47	0.05205	1.41	281.87	0.49
z10	12	1.5	0.60	566	0.3111	1.06	0.043520	0.16	0.47	0.05188	0.99	274.62	0.44
KDPA63													
z5	12	0.9	0.65	279	0.3281	2.27	0.045146	0.28	0.54	0.05273	2.13	284.65	0.78
z2	12	1.2	0.47	357	0.3235	1.63	0.044927	0.21	0.46	0.05224	1.54	283.30	0.59
z3	12	1.1	0.66	1674	0.3205	0.47	0.044778	0.15	0.49	0.05193	0.41	282.38	0.41
z9	12	3.6	0.75	423	0.3192	1.28	0.044657	0.24	0.42	0.05186	1.20	281.63	0.67
z10	12	1.4	0.84	242	0.3173	2.42	0.044612	0.27	0.49	0.05160	2.30	281.36	0.73
z25	12	2.2	0.71	228	0.3176	2.75	0.044514	0.40	0.43	0.05177	2.60	280.75	1.09
z21	12	2.8	0.86	166	0.3104	3.51	0.043484	0.35	0.48	0.05180	3.36	274.39	0.94
Paraná Basin													
RMT													
*z17	8	0.6	0.81	729	0.3316	2.32	0.046218	0.29	0.44	0.05204	2.21	291.26	0.85
*z11	8	0.7	0.75	311	0.3335	1.77	0.046208	0.24	0.39	0.05235	1.69	291.20	0.71
*z18	8	0.4	0.81	767	0.3311	1.13	0.046145	0.39	0.44	0.05204	1.02	290.81	1.13
*z12	8	1.1	0.82	412	0.3307	1.50	0.046122	0.27	0.40	0.05200	1.41	290.67	0.77
*z15	8	0.5	0.79	1197	0.3321	0.63	0.046054	0.22	0.43	0.05230	0.57	290.25	0.63
*z13	8	0.4	0.72	1592	0.3312	0.49	0.046044	0.19	0.45	0.05216	0.44	290.19	0.54
*z16	8	1.0	0.72	825	0.3310	0.78	0.046010	0.28	0.43	0.05217	0.70	289.98	0.80
*z14	8	0.8	0.87	904	0.3284	0.70	0.045762	0.16	0.41	0.05204	0.65	288.45	0.45
z205	12	4.4	0.70	166	0.3317	3.47	0.046207	0.39	0.46	0.05209	3.31	291.19	1.12
z301	12	1.7	0.75	280	0.3190	2.06	0.046078	0.22	0.48	0.05023	1.97	290.40	0.62
z302	12	1.5	0.86	583	0.3307	0.99	0.046163	0.15	0.44	0.05198	0.93	290.92	0.42
z303	12	1.6	0.75	553	0.3293	1.05	0.046183	0.16	0.42	0.05174	0.99	291.05	0.45
z306	12	1.6	0.76	510	0.3453	1.17	0.047962	0.22	0.45	0.05223	1.09	302.00	0.64
z308	12	1.2	0.59	937	0.3322	0.87	0.046203	0.20	0.50	0.05217	0.79	291.17	0.57

ANT.01													
z43	12	2.1	0.97	135	0.3836	4.33	0.051360	0.46	0.48	0.05419	4.13	322.87	1.46
z47	12	1.1	0.86	121	0.3550	5.27	0.049153	0.52	0.48	0.05240	5.04	309.32	1.56
z49	12	2.1	0.61	868	0.3518	0.71	0.048861	0.17	0.44	0.05224	0.65	307.52	0.51
z45	12	3.3	0.35	196	0.3549	2.81	0.048746	0.35	0.45	0.05283	2.67	306.82	1.06
z44	12	1.9	0.70	368	0.3446	1.47	0.048070	0.17	0.50	0.05202	1.39	302.66	0.52
z48	12	1.6	0.72	326	0.3439	1.68	0.047848	0.19	0.49	0.05215	1.59	301.30	0.56
z46	12	1.2	0.68	756	0.3413	1.23	0.047086	0.59	0.56	0.05259	1.02	296.60	1.70
*z10	8	0.3	0.38	2237	0.6865	0.59	0.085655	0.45	0.79	0.05813	0.37	529.79	2.39
*z1	8	3.5	0.47	140	0.6768	3.63	0.084693	0.41	0.46	0.05796	3.46	524.08	2.13
*z11	8	1.1	0.32	29	0.4494	77.86	0.082998	5.59	0.53	0.03926	75.03	513.99	28.71
*z6	8	0.4	0.28	2178	0.6196	0.39	0.078668	0.28	0.77	0.05712	0.25	488.17	1.38
*z4	8	0.6	0.45	1144	0.6059	0.56	0.077419	0.30	0.60	0.05676	0.45	480.70	1.46
*z3	8	2.1	0.24	310	0.5971	1.72	0.076606	0.24	0.45	0.05653	1.63	475.83	1.13
*z134	8	0.7	0.65	234	0.3552	6.63	0.050250	0.55	0.71	0.05126	6.25	316.05	1.73
*z5	8	0.5	0.76	1405	0.3540	0.71	0.048412	0.47	0.71	0.05304	0.50	304.77	1.45
*z101	8	1.7	1.06	177	0.3514	3.30	0.047979	0.39	0.45	0.05312	3.14	302.10	1.17
*z107	8	0.9	0.77	647	0.3410	7.97	0.047911	0.60	0.11	0.05162	7.93	301.69	1.81
*z137	8	0.7	0.93	165	0.3522	3.33	0.047812	0.41	0.43	0.05342	3.18	301.07	1.23
*z7	8	0.4	0.46	851	0.3442	0.77	0.047673	0.16	0.39	0.05236	0.72	300.22	0.47
*z136	8	0.7	0.80	430	0.3476	1.38	0.047635	0.34	0.39	0.05292	1.29	299.99	1.01
*z110	8	1.2	0.76	335	0.3402	1.63	0.047617	0.24	0.37	0.05181	1.56	299.87	0.72
*z138	8	0.4	0.80	592	0.3452	1.07	0.047602	0.20	0.33	0.05259	1.02	299.78	0.59
*z9	8	0.5	0.93	774	0.3438	0.81	0.047600	0.20	0.42	0.05239	0.75	299.77	0.60
*z103	8	1.1	0.70	229	0.3432	2.45	0.047515	0.29	0.45	0.05239	2.34	299.25	0.86
*z2	8	0.6	0.85	457	0.3447	1.26	0.047471	0.24	0.37	0.05267	1.20	298.97	0.71
*z105	8	1.1	0.85	196	0.3417	2.88	0.047435	0.41	0.39	0.05225	2.75	298.76	1.22
*z111	8	0.6	0.74	481	0.3444	1.08	0.047366	0.19	0.38	0.05273	1.03	298.33	0.56
*z8	8	1.5	0.92	197	0.3445	3.74	0.047212	0.59	0.43	0.05292	3.53	297.38	1.75
*z106	8	1.8	0.76	256	0.3226	4.16	0.047060	0.64	0.40	0.04972	3.95	296.45	1.91
*z135	8	1.3	0.69	222	0.3374	3.05	0.047001	0.58	0.32	0.05206	2.91	296.08	1.72
AWT													
*z3	8	0.5	0.88	1639	5.9716	1.65	0.357084	1.62	0.98	0.12129	0.33	1968.34	31.83
*z2	8	0.5	0.79	1932	1.7494	0.45	0.172314	0.36	0.83	0.07363	0.25	1024.85	3.73
*z1	8	0.7	0.64	1742	1.7353	0.33	0.171472	0.22	0.74	0.07340	0.22	1020.22	2.24
*z5	8	0.6	0.83	2967	0.8113	1.12	0.098183	1.07	0.96	0.05993	0.31	603.75	6.47
*z7	8	0.6	0.78	3231	0.6907	1.72	0.086133	1.70	0.99	0.05816	0.27	532.63	9.04
*z6	8	0.5	0.82	642	0.3426	1.21	0.047001	0.25	0.38	0.05287	1.13	296.08	0.75
*z4	8	0.5	0.39	1526	0.3375	0.56	0.046795	0.21	0.44	0.05231	0.50	294.82	0.62

a Total mass of common Pb.

b Th contents calculated from radiogenic ^{208}Pb and ^{230}Th-corrected $^{206}Pb/^{238}U$ date of the sample, assuming concordance between U-Pb Th-Pb systems.

c Measured ratio corrected for fractionation and spike contribution only.

d Measured ratios corrected for fractionation, tracer and blank.

e Isotopic dates calculated using λ^{238} = 1.55125E-10 (Jaffey et al. 1971) and λ^{235} = 9.8485E-10 (Jaffey et al. 1971).

f Corrected for initial Th/U disequilibrium using radiogenic ^{208}Pb and Th/U[magma] specified. Deficient radiogenic ^{206}Pb due to initial deficit of ^{230}Th is accounted for by assuming a partition coefficient ratio DTh/DU of 0.2 (as applied in Wotzlaw et al., 2014).

* Samples spiked with the BGC 535 tracer solution.

CA – chemical abrasion time

Fig. A1

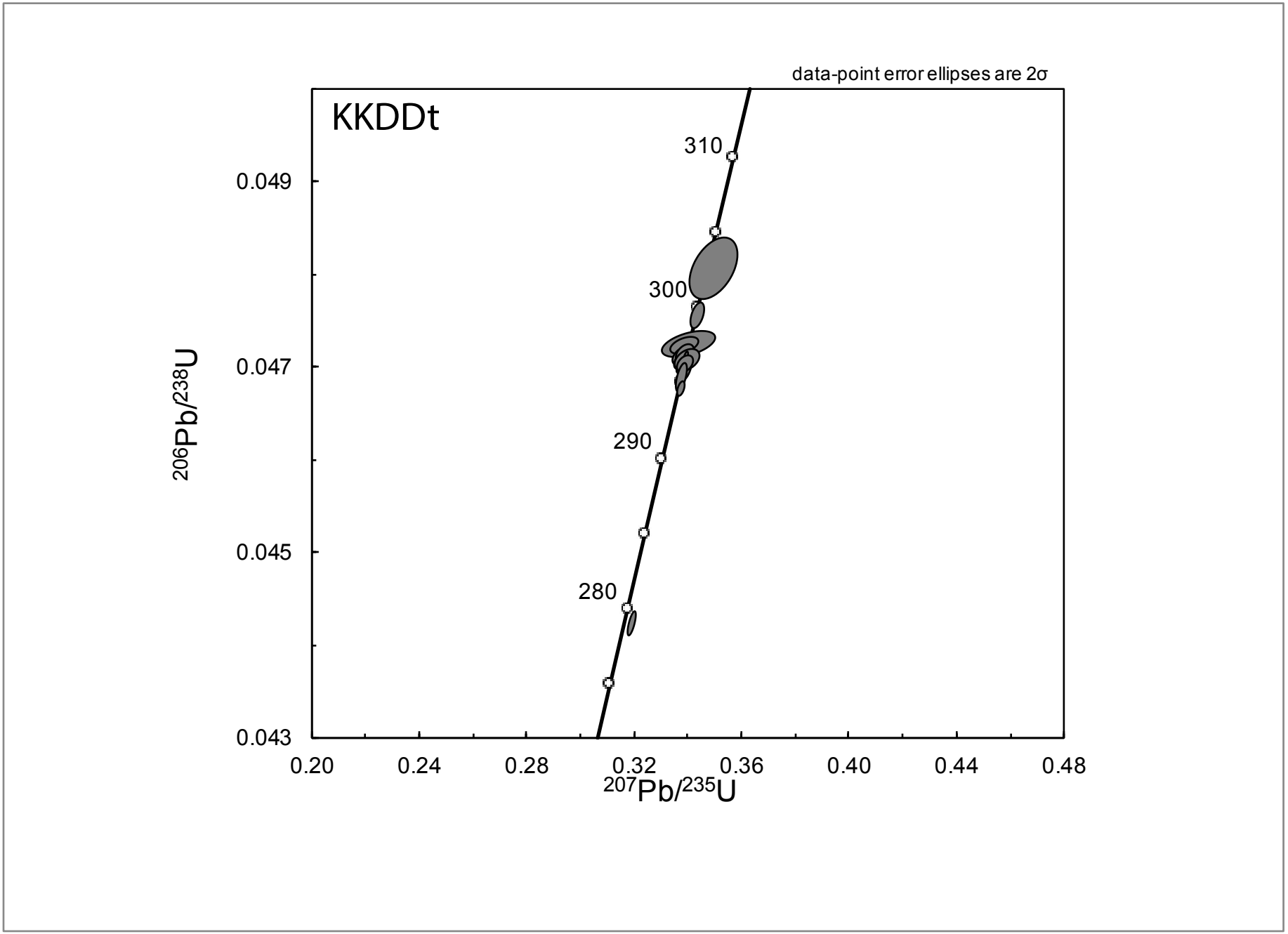
data-point error ellipses are 2σ
KKDDt
310
300
290
280
0.049
0.047
0.045
0.043
$^{206}Pb/^{238}U$
0.20
0.24
0.28
0.32
0.36
0.40
0.44
0.48
$^{207}Pb/^{235}U$

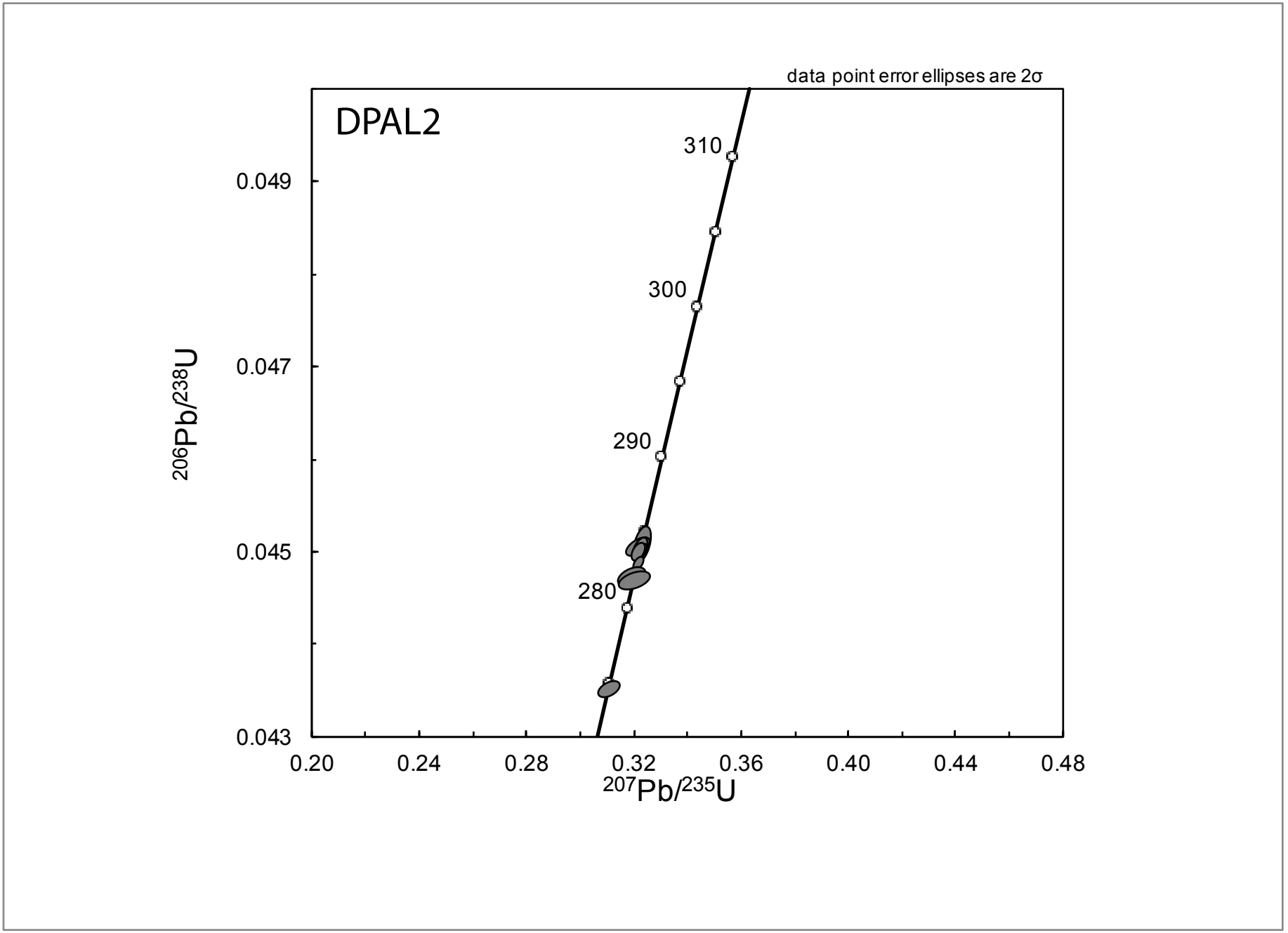
data point error ellipses are 2σ
DPAL2
310
300
290
280
0.049
0.047
0.045
0.043
$^{206}Pb/^{238}U$
0.20
0.24
0.28
0.32
0.36
0.40
0.44
0.48
$^{207}Pb/^{235}U$

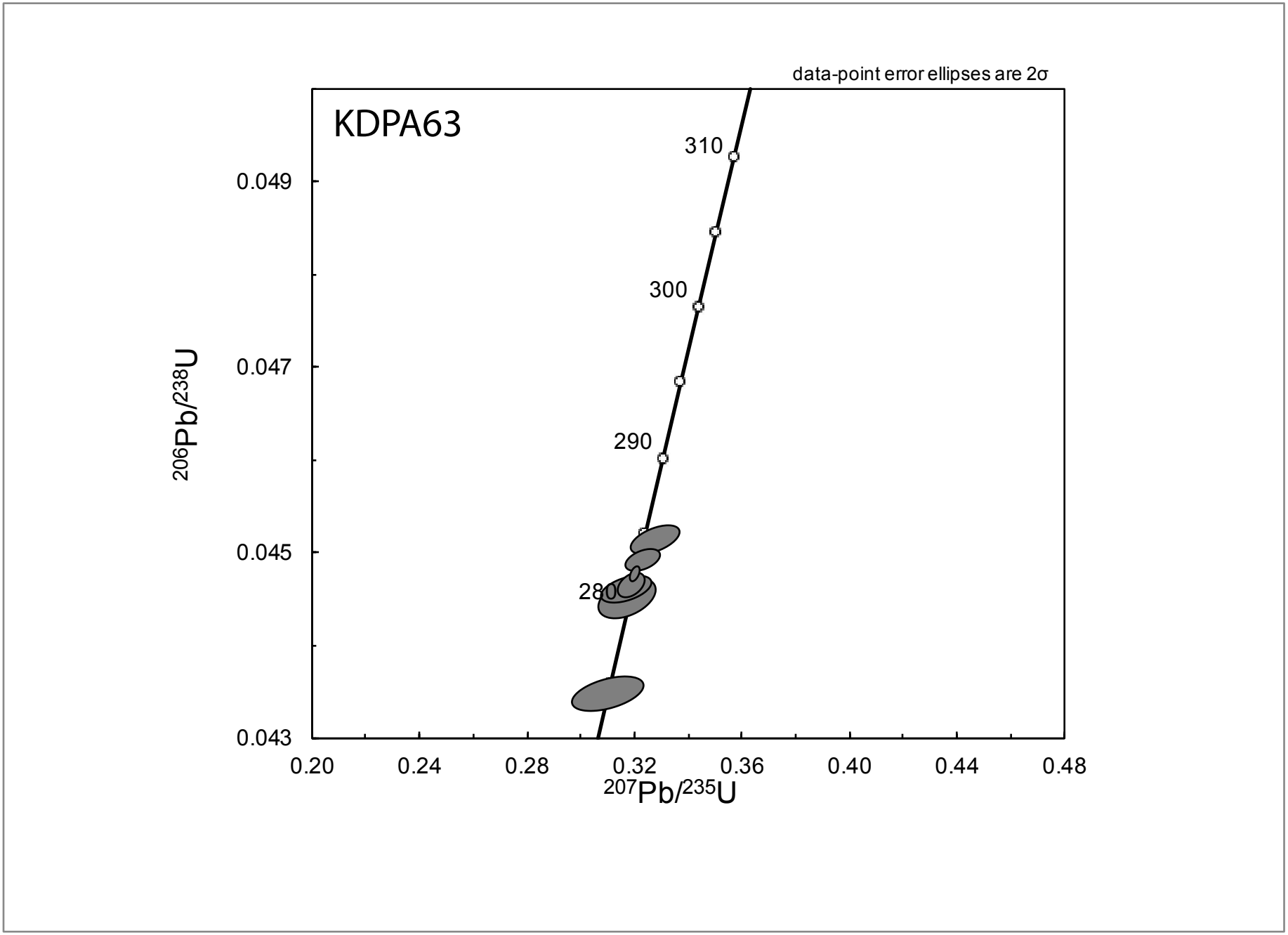
data-point error ellipses are 2σ
KDPA63
310
300
290
280
0.049
0.047
0.045
0.043
$^{206}Pb/^{238}U$
0.20
0.24
0.28
0.32
0.36
0.40
0.44
0.48
$^{207}Pb/^{235}U$

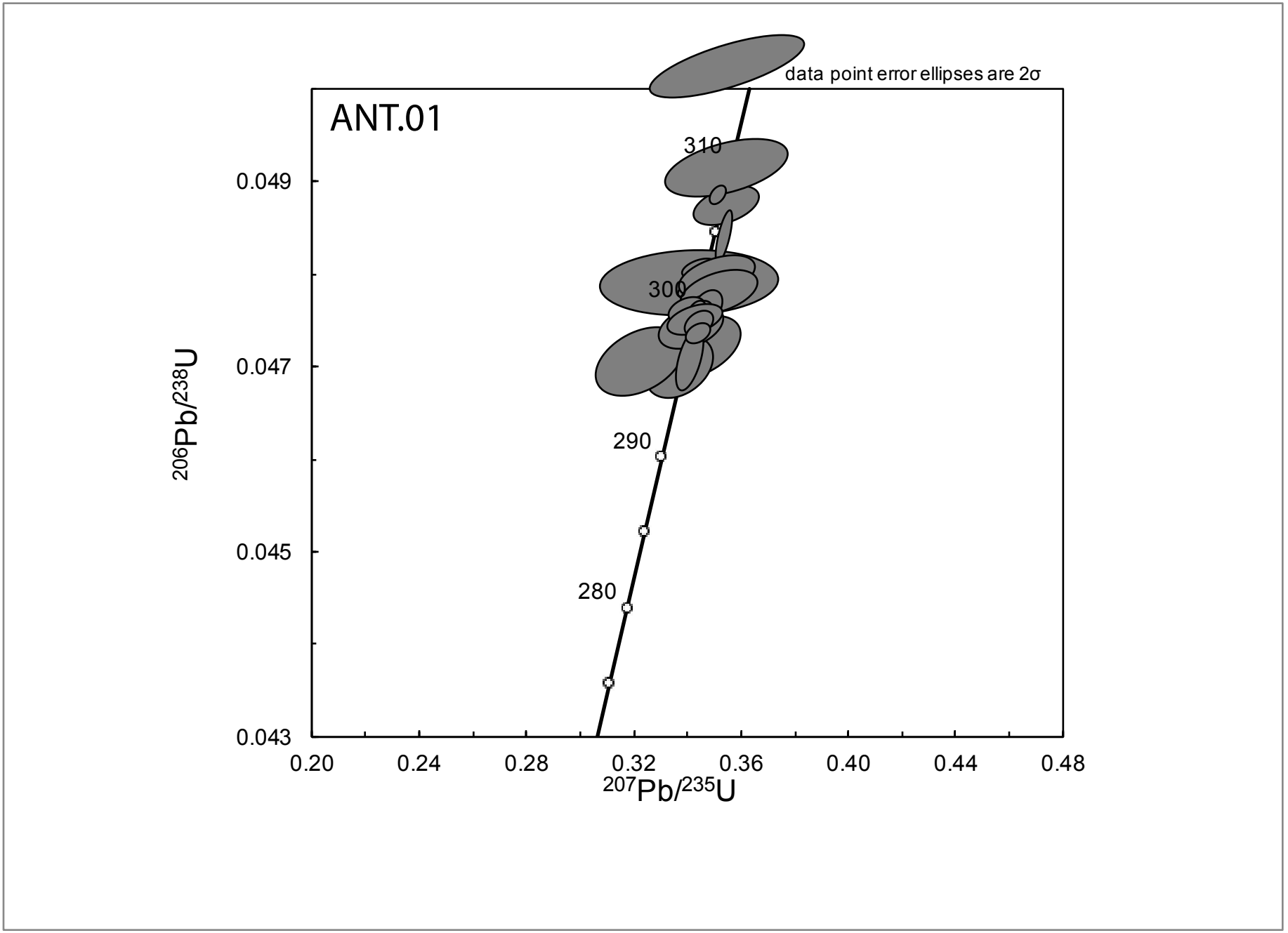
ANT.01
data point error ellipses are 2σ
310
300
290
280
0.049
0.047
0.045
0.043
0.20
0.24
0.28
0.32
0.36
0.40
0.44
0.48
206Pb/238U
207Pb/235U

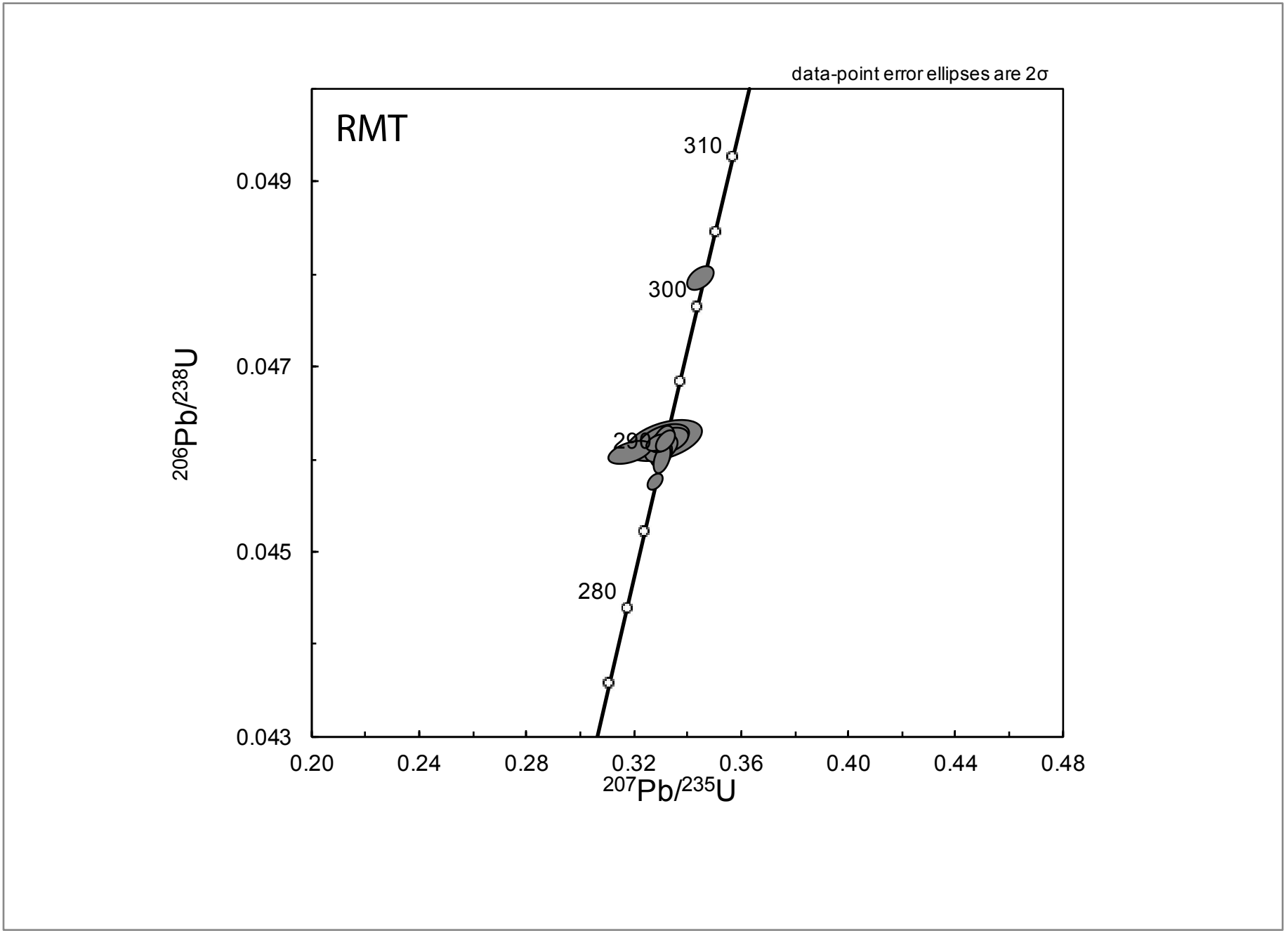
data-point error ellipses are 2σ
RMT
310
300
290
280
0.049
0.047
0.045
0.043
0.20
0.24
0.28
0.32
0.36
0.40
0.44
0.48
206Pb/238U
207Pb/235U

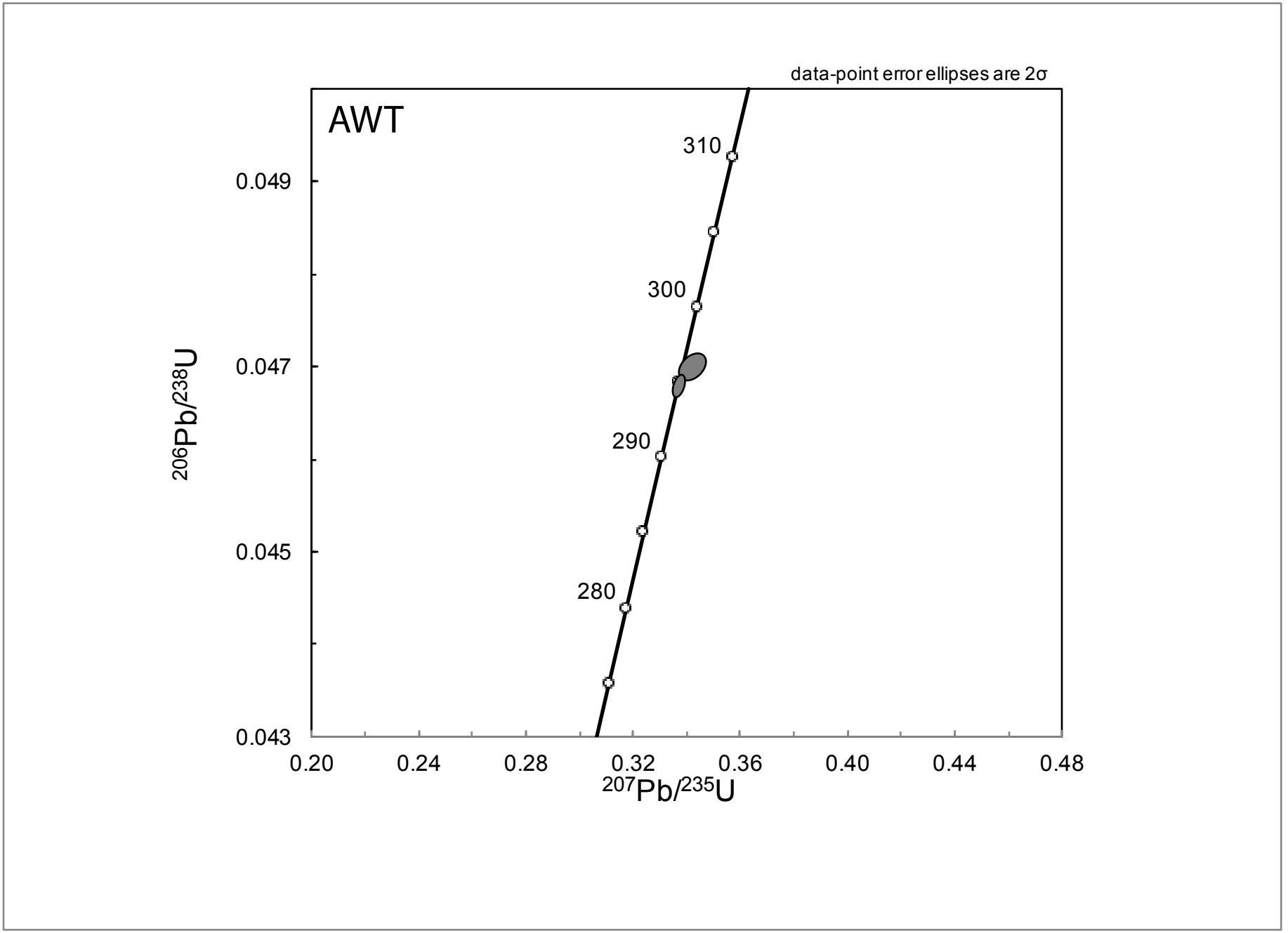
data-point error ellipses are 2σ
AWT
310
300
290
280
0.049
0.047
0.045
0.043
$^{206}Pb/^{238}U$
0.20
0.24
0.28
0.32
0.36
0.40
0.44
0.48
$^{207}Pb/^{235}U$

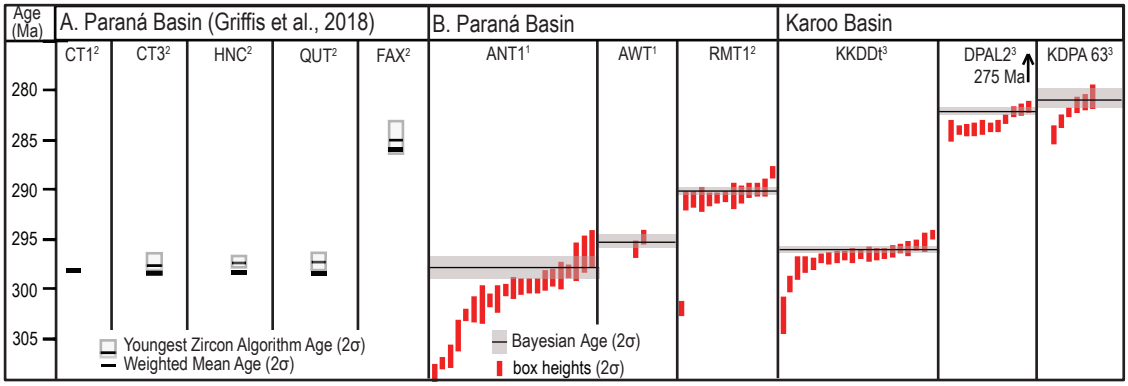
Age (Ma)
A. Paraná Basin (Griffis et al., 2018)
B. Paraná Basin
Karoo Basin
CT1²
CT3²
HNC²
QUT²
FAX²
ANT1¹
AWT¹
RMT1²
KKDDt³
DPAL2³
275 Ma
KDPA 63³
280
285
290
295
300
305
Youngest Zircon Algorithm Age (2σ)
Weighted Mean Age (2σ)
Bayesian Age (2σ)
box heights (2σ)

Fig. A2